J-PARC-PAC 2025-7
*D*raft version 2.0

Proposal for J-PARC 50 GeV Proton Synchrotron

J/ψ Production in $\pi^- p$ Reaction near Threshold

Spokesperson	Sun Young Ryu (RCNP, The University of Osaka)
Beam line	π20
Beam	π^- / 8.2–11.0 GeV/c (from threshold to $W = 4.64$ GeV) in 0.02 GeV intervals
Beam Intensity	1×10^8/ spill (2 s spill duration)
Target	Liquid hydrogen (570 mm in length)
Reaction	$\pi^- p \to J/\psi n$
Detector	E50 Detector + Forward detector components
Beam time	50 days
Expected yield	7.5×10^3 events

July 13, 2025

The J/ψ Collaboration

Sun Young Ryu (*Spokesperson*),
Kotaro Shirotori, Hiroyuki Noumi, Takatsugu Ishikawa,
Ken Suzuki, Keigo Mizutani
RCNP, The University of Osaka, Osaka, Japan

Jung Keun Ahn, Woo Seung Jung
Korea University, Seoul, Korea

Igor Strakovsky
The George Washington University, United States

Hyun-Chul Kim
Inha University, Incheon, Korea

Samson Clymton
APCTP, Pohang, Korea

Seung-il Nam
Pukyong National University, Busan, Korea

Sang Ho Kim
Soongsil University, Seoul, Korea

and

High-p Beam Line Collaboration

Abstract

We propose a new experiment to study J/ψ production in $\pi^- p$ reactions near the threshold at the π20 beam line. Investigating J/ψ production in the π^-p reaction will provide valuable insights into the nature of $c\bar{c}$ pair creation in pion-induced reactions, particularly regarding hidden-charm pentaquark states.

We plan to measure the total cross sections for the exclusive $\pi^- p \rightarrow J/\psi n$ reaction near the threshold using the E50 spectrometer with the addition of forward detector components. We will prepare our experimental setup in close collaboration with the high-p Collaborations.

This measurement aims to provide the world's first data on π^--induced J/ψ production reaction near the threshold. We are requesting 50 days of beam time for the energy scan. If we discover new structures related to exotic pentaquark states, we will seek an additional 50 days to investigate pentaquark searches at finer energy intervals.

1 Introduction

The proposed experiment will investigate the J/ψ production in $\pi^- p$ reaction from the threshold ($p = 8.2$ GeV/c) to a center-of-mass energy of $W = 4.63$ GeV (11 GeV/c). This $\pi^- p \to J/\psi n$ reaction provides an excellent opportunity to investigate the dynamics of gluons in hadrons. In the context of the J/ψ production in πN collisions, the violation of the Okubo-Zweig-Iizuka (OZI) rule directly relates to the production of the hidden charm, specifically the $c\bar{c}$ component present in the nucleon.

The observation of hidden-charmed pentaquark states, referred to as $P_{c\bar{c}}$, provides valuable insights into the hadronic structure with a multiquark configuration. However, $P_{c\bar{c}}$ states have only been detected in the decays of bottom-quark hadrons, such as Λ_b and B_s. A recent measurement of J/ψ photoproduction from GlueX has reported no evidence for $P_{c\bar{c}}$ states but has shown intriguing lineshapes that exhibit dip and cusp structures near the mass thresholds of open-charm meson-baryon states.

The absence of $P_{c\bar{c}}$ signals is interpreted as a result of the weak coupling in $J/\psi N$ elastic scattering. Assuming the vector meson dominance in photoproduction, the $\gamma p \to J/\psi p$ reaction process is believed to primarily originate from the $J/\psi p$ elastic channel. In contrast, the π^--induced reaction may dominate the inelastic channel associated with open-charm states. According to a recent theoretical calculation using a comprehensive coupled-channel approach, this inelastic channel might enhance the signals of $P_{c\bar{c}}$ states. Additionally, the $\pi^- p$ reaction warrants further investigation for the search of isospin partners of the $P_{c\bar{c}}$ states.

Reaction	Threshold (GeV/c)
$\gamma p \to J/\psi p$	8.21
$\pi^- p \to J/\psi n$	8.20
$\pi^- p \to J/\psi p \pi^-$	8.81
$K^- p \to J/\psi p K^-$	10.32
$K^+ p \to J/\psi p K^+$	10.32
$\bar{p} p \to J/\psi p \bar{p}$	12.21

Table 1: Threshold beam energy or momentum for J/ψ production.

The $J/\psi N$ interaction can be explored through formation and production reactions using various beam particles, including photons, pions, kaons, and antiprotons. The threshold energy and momentum for different reactions are detailed in Table 1. When using photon and pion beams, we can search for $P_{c\bar{c}}$ states by examining the total cross-section plot of the formation processes. Conversely, other reactions induced by beam particles allow us to investigate the $P_{c\bar{c}}$ states in the $J/\psi N$ invariant mass spectrum. For example, the reaction $K^- p \to J/\psi p K^-$ results in the same final state as the decay process $\Lambda_b \to J/\psi p K^-$.

One advantage of the K^--induced reaction is that it allows for measurements to be taken at varying beam momenta, enabling the exploration of background processes across different phase spaces. with the total center-of-mass energy.

Despite its significant impact on physics, there have been no reported observations of J/ψ production events to date. Upper limits for the reaction $\pi^- p \to J/\psi n$ have been set at approximately 1 nb. Recently, the GlueX Collaboration reported total cross sections for J/ψ production through photoproduction, covering a beam energy range from threshold to 11.5 GeV, with values between a few tens of pb to 1 nb.

Comparatively, the π^--induced reactions are predicted to yield larger cross sections. However, the current upper limits for the π^--induced reactions are comparable to or even smaller than the photoproduction cross sections near the threshold.

Soon, a high-momentum pion beam will become available at J-PARC. This presents an opportunity, making the $\pi^- p \to J/\psi n$ reaction an ideal candidate for searching for isospin partners of hidden-charm pentaquark states.

This proposal will review theoretical predictions and previous experimental results in Section 2. Detailed information about the experiment is provided in the following section. The beam time request is summarized in Section 4, and the current status of the experiment and costs are briefly discussed in Section 5. Section 6 summarizes the experimental proposal.

2 Physics Motivation

2.1 Hidden-Charm Pentaquark States

Significant progress has been made in understanding the underlying theory of the strong interaction, known as Quantum Chromodynamics (QCD), particularly in its perturbative regime. However, much remains to be explored in the non-perturbative regime, especially in the area dominated by the gluonic exchanges and interactions. These strong gluonic field configurations and interactions contribute to most of the mass of nucleons and nuclei. Fundamental approaches like lattice QCD and effective field theories could provide insights into the confinement of hadrons and potentially predict new phenomena in strong interactions.

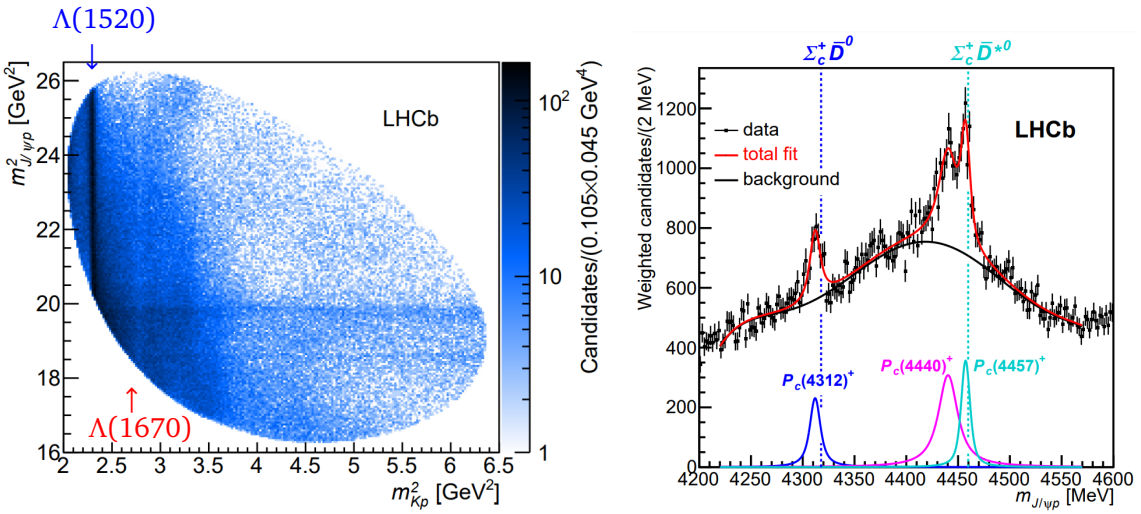

Figure 1: (a) Dalitz plot of the K^-p and $J/\psi p$ mass systems for $\Lambda_b \to J/\psi K^- p$ decay, and (b) its $J/\psi p$ mass spectrum overlaid with extracted lineshapes of $P_{c\bar{c}}$ states.

State	M (MeV)	Γ (MeV)	$\mathscr{R}$ (%)
$P_{c\bar{c}}(4312)^+$	$4311.9 \pm 0.7^{+6.8}_{-0.6}$	$9.8 \pm 2.7^{+3.7}_{-4.5}$	$0.3 \pm 0.07^{+0.34}_{-0.09}$
$P_{c\bar{c}}(4440)^+$	$4440.3 \pm 1.3^{+4.1}_{-4.7}$	$20.6 \pm 4.9^{+8.7}_{-10.1}$	$1.11 \pm 0.33^{+0.22}_{-0.10}$
$P_{c\bar{c}}(4457)^+$	$4457.3 \pm 0.6^{+4.1}_{-1.7}$	$6.4 \pm 2.0^{+5.7}_{-1.9}$	$0.53 \pm 0.16^{+0.15}_{-0.13}$

Table 2: Properties of hidden-charm pentaquark states.

The observation of peaking structures in the $J/\psi p$ mass spectrum reported by the LHCb Collaboration, currently referred to as hidden-charm pentaquark state, has sparked interest in exotic hadron spectroscopy [1]. These $P_{c\bar{c}}$ states were found in the $\Lambda_b \to J/\psi p K^-$ decay. In the analysis, a prominent horizontal band is observed across the entire mass

range of K^-p mass, which overlaps with two distinct vertical bands associated with the $\Lambda(1520)$ and $\Lambda(1670)$ resonances, as illustrated in Fig. 1(a).

While the exact nature of $J/\psi p$ states is still a topic of discussion – ranging from resonances and molecular bound states near thresholds to compact pentaquark states – three $P_{c\bar{c}}$ states have been firmly established in the Λ_b decay, summarized in Table 2.

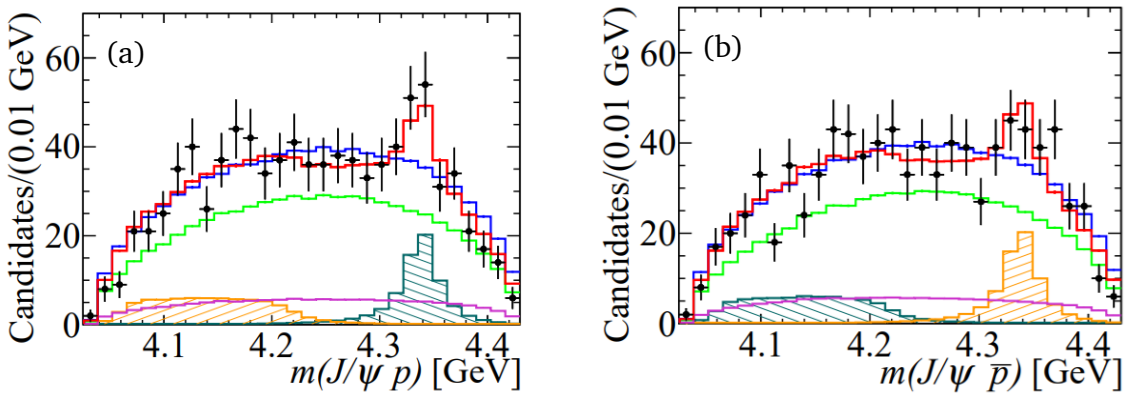

Figure 2: A new structure is seen in (a) the $J/\psi p$ and (b) $J\psi\bar{p}$ mass spectra with a mass of $4.337^{+7}_{-4} \pm 2$ MeV and width of $29^{+26}_{-12} \pm 14$ MeV in flavor-untagged $B^0_s \to J/\psi p\bar{p}$ decays.

Recently, the same experimental group reported evidence for a new structure in the $J/\psi p$ and $J\psi\bar{p}$ systems with a mass of $4.337^{+7}_{-4} \pm 2$ MeV and width of $29^{+26}_{-12} \pm 14$ MeV in flavor-untagged $B^0_s \to J/\psi p\bar{p}$ decays [2], as illustrated in Fig. 2(a) and (b). However, no evidence is seen for either a $P_{c\bar{c}}$ at a mass of 4312 MeV or the glueball state $f_J(2220)$.

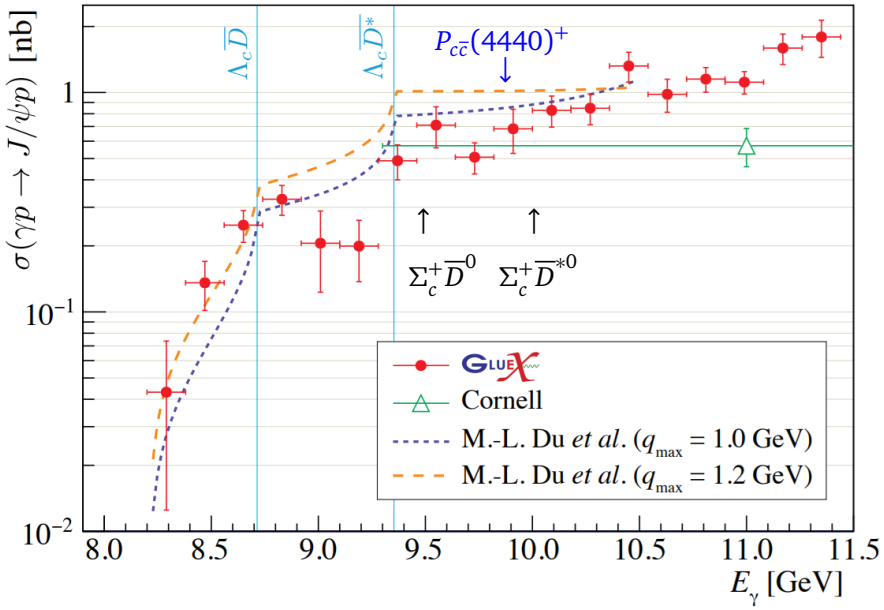

Figure 3: Total cross sections for $\gamma p \to J/\psi p$ reaction near the threshold [3].

In contrast, J/ψ photoproduction cross sections near the threshold show no evidence for the hidden-charm pentaquarks at their original mass locations. However, there are intriguing structures near the mass thresholds for open-charm channels involving $\Lambda_c\bar{D}$ and $\Lambda_c\bar{D}^*$, as illustrated in Fig. 3. Theoretical models for open charm coupled-channel mechanism predict a cusp-like behavior [6], as shown in Fig. 4(a). Fig. 5 represents J/ψ photoproduction mechanisms which include vector-meson dominance model, open-charm channel production, and coupled-channel diargams. The near-threshold J/ψ photoproduction could be dominated by loops with open charm hadrons such as $\Lambda_c\overline{D}^{(*)}$. Additionally, the possible observation of the $P_{c\bar{c}}(4312)^+$ state is discussed based on a sharp dip structure about 77 MeV below the LHCb mass [4], as depicted in Fig. 4(b).

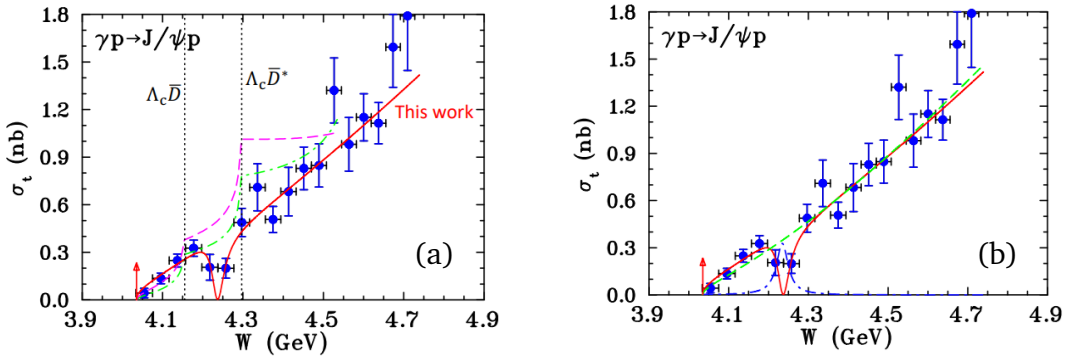

Figure 4: Cusp-like behavior in the total cross sections for J/ψ photoproduction process is fitted with (a) the open-charm model calculation (green and magenta curves) and (b) a sharp dip structure about 77 MeV below the $P_{c\bar{c}}(4312)^+$ mass.

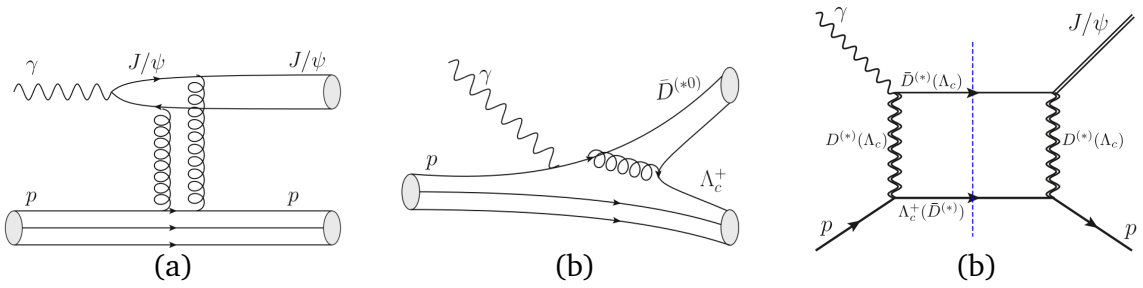

Figure 5: (a) Vector-meson dominance model mechanism for the near-threshold J/ψ photoproduction, (b) $J\psi$ photoproduction through $\Lambda_c\bar{D}^{(*)}$ which then rescatter into J/ψ, and (c) Feynman diagram for the coupled-channel mechanism.

The elastic cross section for the $J/\psi N$ elastic channel is significantly smaller than that of six inelastic channels, such as $\Lambda_c^{(*)}\overline{D}^{(*)}-J/\psi N$ and $\Sigma_c^{(*)}\overline{D}^{(*)}-J/\psi N$. The near-threshold J/ψ photoproduction may suppress the $P_{c\bar{c}}$ states due to the interference effect in an off-shell coupled-channel formalism approach [7], as depicted in Fig. 6(a). The $P_{c\bar{c}}$ production cross sections for $J/\psi N$ elastic channels with positive and negative parities are 10^2 to 10^3

smaller than those for inelastic channels. This suppression of the $J/\psi N$ elastic channel contribution leads to no distinct structures for $P_{c\bar{c}}$ states in the total cross section for near-threshold J/ψ photoproduction reaction.

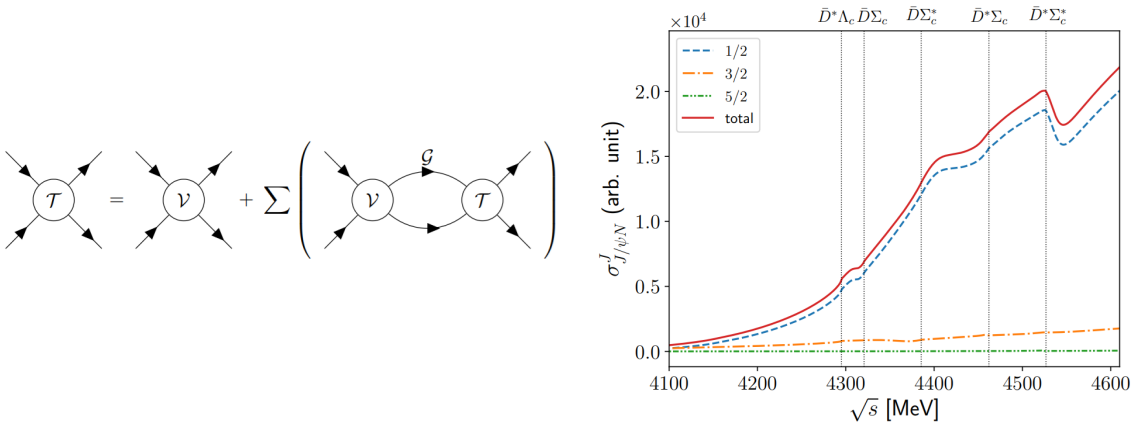

(a) (b)

Figure 6: (a) Diagrams in an off-shell coupled-channel approach, and (b) the calculated cross sections for the near-threshold J/ψ photoproduction with different spin values of $P_{c\bar{c}}$ states.

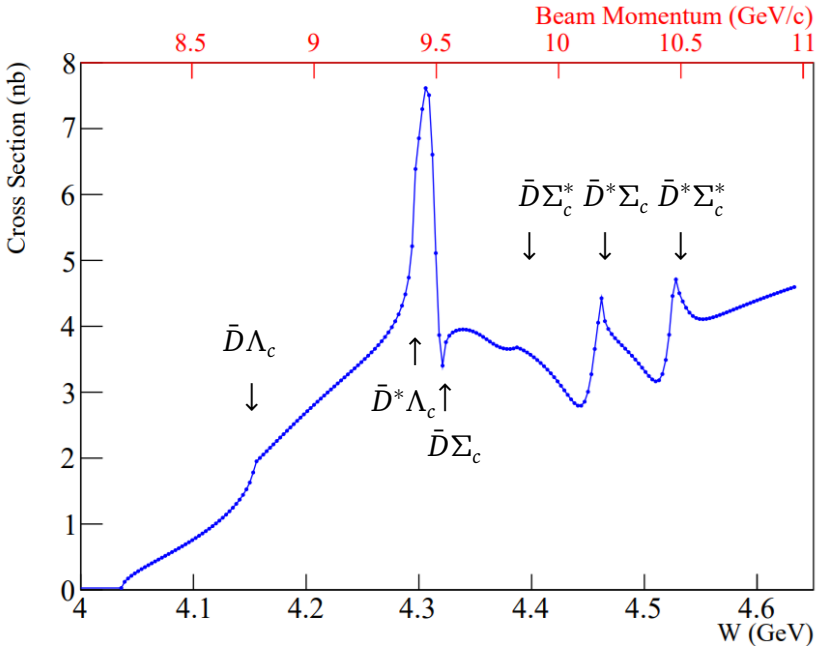

Figure 7: Calculated total cross sections for $\pi^- p \to J/\psi n$ reaction in a full coupled-channel formalism.

This new coupled-channel approach predicts a distinct peaking structure for the $P_{c\bar{c}}(4312)^0$ state and cusp-like structures near six mass thresholds in total cross sections

for the $\pi^- p \to J/\psi n$ reaction from threshold to $W = 4.65$ GeV, as illustrated in Fig. 7. The differential cross sections exhibit significant variation with the π^- beam momentum, as shown in Fig. 8, This variation is due to the drastic changes in total cross sections resulting from the emergence of $P_{c\bar{c}}$ states and cusp-like structures.

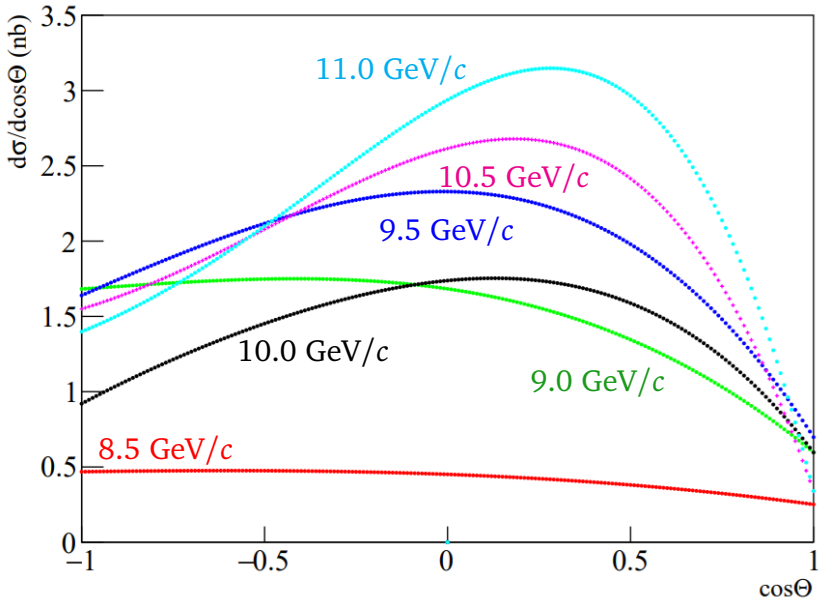

Figure 8: Calculated differential cross sections for $\pi^- p \to J/\psi n$ reaction in a full coupled-channel formalism.

2.2 Past Measurements of the $\pi^- p \to J/\psi n$ Reaction

To date, there have been no observations of exclusive J/ψ production events in the $\pi^- p$ reaction. Only upper limits for the process $\pi^- p \to J/\psi n$ have been established by two older experiments.

One experiment utilized a 13 GeV/c pion beam and a plastic scintillator target [8]. The single event sensitivity was determined to be 3.3 pb. An upper limit on the exclusive J/ψ production cross section, when multiplied by the branching ratio into e^+e^-, was found to be 7.6 pb at 13 GeV/c. The latest branching ratio value for $J/\psi \to e^+e^-$ is 5.971%[5], which implies an upper limit on exclusive J/ψ production of 127 pb. This result differs from the previously reported value of 103 pb in the literature, which was based on an older branching ratio. This upper limit calculation is based on the assumption that there are 3.3 effective protons in the carbon nuclei of the scintillator target, which introduces additional uncertainties into the upper limit.

The other experiment utilized a liquid hydrogen target with a weighted mean momentum of 8.75 GeV/c [9]. The researchers observed no events consistent with the reaction

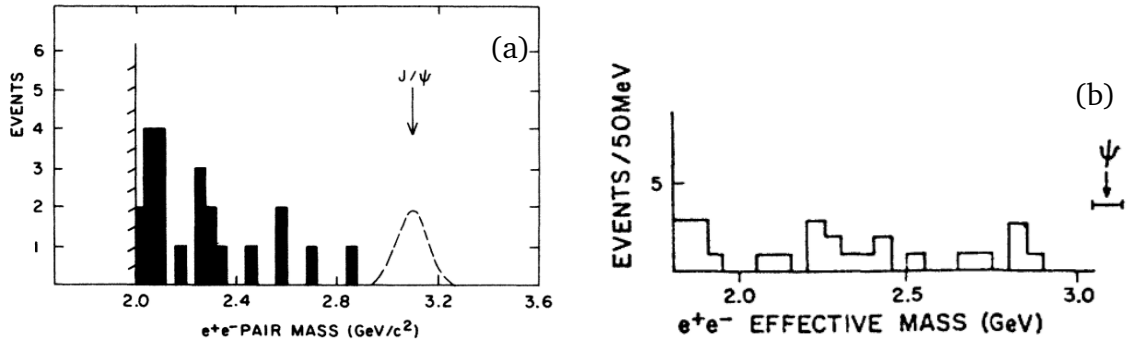

Figure 9: (a) Invariant mass spectrum of e^+e^- in the $\pi^- p \to J/\psi n$ reaction at 13 GeV/c and (b) the e^+e^- mass spectrum at 8.7 GeV/c.

$\pi^- p \to J/\psi n$ and established an upper limit of 1.3 nb[1] (90% confidence level) for the total cross section.

While π^--induced reactions are predicted to result in larger cross sections, the current upper limits for these reactions are comparable to, or even smaller than, the photoproduction cross sections near the threshold, which range from a few tens of pb to 1 nb in photon beam energies between 8.2 and 11.5 GeV.

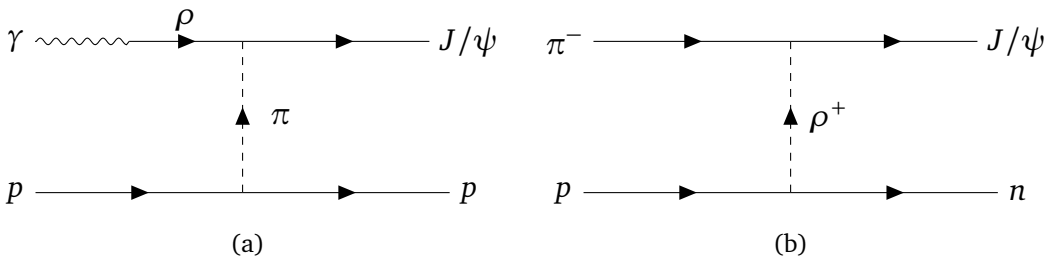

Figure 10: (a) J/ψ photoproduction process through γ-ρ coupling and π exchange in the t channel, and (b) J/ψ production in the $\pi^- p$ reaction via ρ^+ exchange in the t channel.

The photoproduction of J/ψ from the proton involves the coupling of a photon to a ρ vector meson. This meson then interacts with the proton through the exchange of a π^0 in the t channel. In contrast, pion-induced J/ψ production can occur via ρ exchange in the t channel, as illustrated in Fig. 10. The coupling of $J/\psi\rho\pi$ is included in the diagram for both photoproduction and π^--induced reactions. This coupling is significant, as evidenced by the branching ratio for the $J/\psi \to \rho\pi$ decay, which is 1.88%. Additionally, the decay into a specific charge mode, $\rho^0\pi^0$, accounts for one-third of the total branching ratio.

The lack of J/ψ observation in the $\pi^- p \to J/\psi n$ reaction supports a proposal for the first measurement of exclusive J/ψ production cross sections in the $\pi^- p$ reactions near the

[1]The original paper reported a value of 1.1 nb, assuming 7% of the branching ratio for the decay $J/\psi \to e^+e^-$.

threshold. This new measurement aims to provide valuable insights into the production mechanism of J/ψ in the $\pi^- p$ reaction as well as to facilitate the search for $P_{c\bar{c}}$ states.

2.3 Reaction Mechanism of J/ψ Production Processes

The production of J/ψ in hadronic reactions is an extremely sensitive tool for studying the Okubo-Zweig-Iizuka (OZI) rule. The OZI rule specifies a vanishing amplitude for processes represented by disconnected quark diagrams. Thus, a violation of the OZI rule might be regarded as evidence for a hidden $q\bar{q}$ component in the initial hadrons. In case of the J/ψ production in πN collisions the OZI violation directly leads to the percentage of the $c\bar{c}$ component in the nucleon, or hidden charm.

The π^--induced reaction can facilitate the search for isospin partners of hidden-charm pentaquark states, denoted as $P_{c\bar{c}}$. Due to isospin symmetry, we have the following relationships:

$$\sigma(\pi^0 p \to J/\psi p) = \sigma(\pi^0 n \to J/\psi n) = \frac{1}{2}\sigma(\pi^- p \to J/\psi n) = \frac{1}{2}\sigma(\pi^+ n \to J/\psi p).$$

This isospin relation suggests that the $\pi^+ d \to J/\psi pp$ reaction would have a cross section similar to that of the $\pi^- p \to J/\psi n$ reaction. It is important to note that the $\pi^+ p$ interaction with a proton in a deuteron cannot contribute to the J/ψ production.

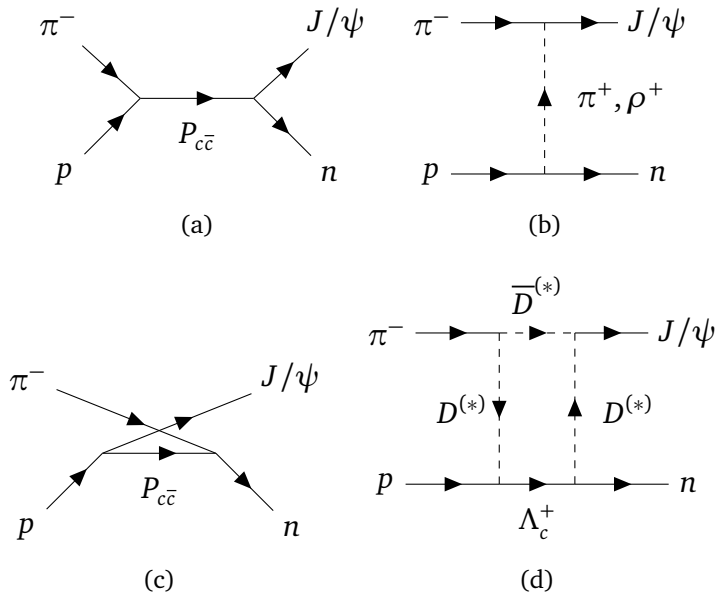

Figure 11: Relevant Feynman diagrams for J/ψ production in $\pi^- p$ reaction through (a) s-channel, (b) t-channel, (c) u-channel, and (d) rescattering diagrams.

There are several theoretical predictions for the near-threshold cross sections of the

$\pi^- p \to J/\psi n$ reaction, compared to the upper limits established by experiments. Sibirtsev and Tsushima calculated the total cross section for $\pi^- N \to J/\psi N$ using t-channel ρ-exchange in an effective Lagrangian approach. By applying the value for the $g_{J/\psi\rho\pi} = 6.78 \times 10^{-3}$, they estimated the maximum cross section to be 140 pb at 12 GeV/c [10], as illustrated in Fig. 12(a).

Lü *et al.* also investigated the $\pi^- p \to J/\psi n$ within an effective Lagrangian framework to search for the neutral $P_{c\bar{c}}$ states [11]. They assumed that the background contribution primarily arises from t-channel π and ρ exchanges. Their theoretical calculations indicate significant divergences from the background contributions, exhibiting clear peak structures corresponding to the $P_{c\bar{c}}$ states. This theoretical study yields a total cross section of 1 μb at 4.38 GeV and 4.45 GeV, as shown in Fig. 12(b).

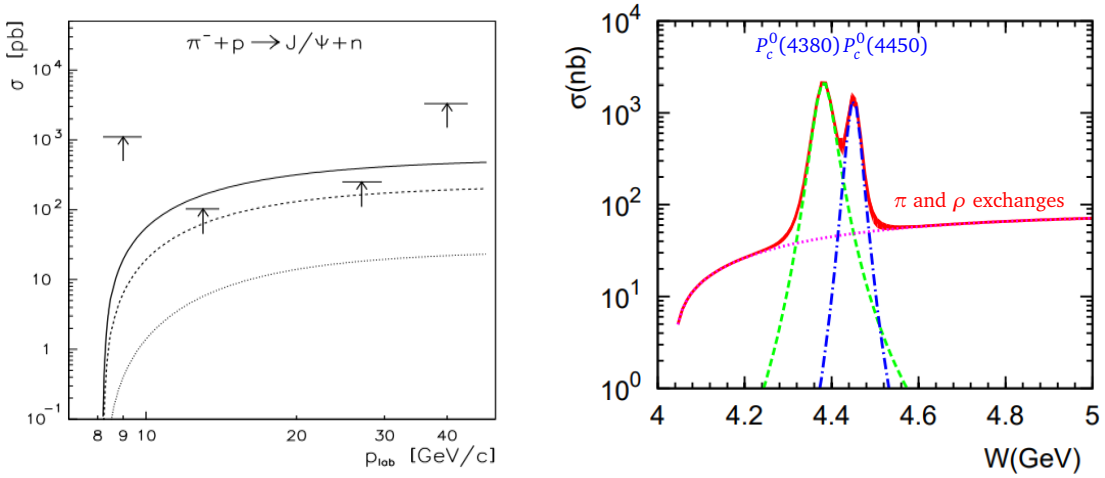

Figure 12: (a) The total cross section for the $\pi^- p \to J/\psi n$ reaction [10]. Arrows indicates the upper limits from experimental data extracted from πA collisions. Curves represent the calculation results with different cut-off parameters: $\Lambda = 1$ GeV (dotted), $\Lambda = 2$ GeV (dashed), and without the form factor at the $J\psi\rho\pi$ vertex (solid). (b) The total cross section for the $\pi^- p \to J/\psi n$ reaction with $J^P = (5/2^+, 3/2^-)$ assumption for $(P_{c\bar{c}}(4380)^0, P_{c\bar{c}}(4450)^0)$, respectively [11].

Wu and Lee developed a coupled-channel model comprising three channels involving πN, ρN, and $J/\psi N$ to predict the $\pi N \to J/\psi N$ cross sections [12]. The strength of the $J/\psi N$ interaction is parametrized using a Yukawa form: $v_{J/\psi N, J/\psi N} = -\alpha \frac{e^{-\mu r}}{r}$. This is related to $J/\psi N$ scattering length and depends on the parameters α and μ. With $\mu = 0.60$, the scattering length ranges from -0.05 fm when $\alpha = 0.06$ to -8.83 fm when $\alpha = 0.60$. The calculated total cross sections for $\pi^- p \to J/\psi n$ are illustrated in Fig. 13(a).

Kim *et al.* investigated J/ψ production in the $\pi^- N$ reaction based on a hydridized Regge model [13]. They considered the process involving π and ρ exchange in the t channel as background contributions. This background cross section was estimated to be on the order of 0.1 to 1 pb, guided by the experimental upper limits. In contrast, the

total cross section near the $P_{c\bar{c}}$ masses reaches approximately 1 nb. This theoretical work predicts cross sections that are three orders of magnitude smaller than those reported by Lü *et al.*

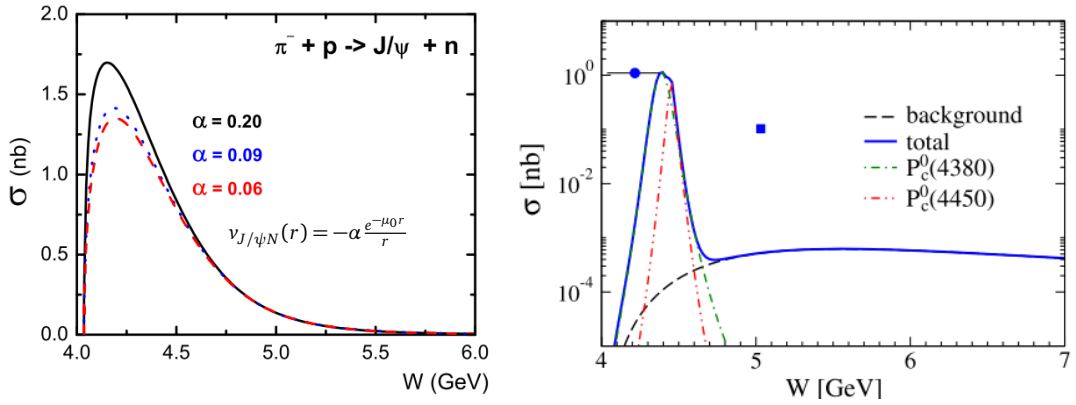

Figure 13: (a) Total cross sections of $\pi^- p \to J/\psi n$ reaction from a coupled channel model calculation involving πN, ρN, and $J/\psi N$ channels. Curves represents the results with different α values [12]. (b) Total cross sections for $\pi^- p \to J/\psi n$ reaction with $J^P = (5/2^+, 3/2^-)$ assignment for $(P_{c\bar{c}}(4380)^0, P_{c\bar{c}}(4450)^0)$, based on a hybridized Regge model [13].

Current theoretical approaches predict significantly different cross sections for the $\pi^- p \to J/\psi n$ reaction near threshold, as summarized in Table 3. This discrepancy arises from differing treatments of experimental upper limits. Some model calculations consider these upper lmits as the maximum total cross sections due to the emergence of $P_{c\bar{c}}$ states. In contrast, other models interpret these limits as the minimum cross sections for the $\pi^- p \to J/\psi n$ reaction in the absence of $P_{c\bar{c}}$ states.

Reference	$\sigma(W = 4.4$ GeV)	Reference	$\sigma(W = 4.4$ GeV)
A. Sibirtsev *et al.*[10]	$\sim$ 50 pb	Q.-F. Lü *et al.*[11]	$\sim$ 50 nb
J.-J. Wu *et al* [12]	$\sim$ 1.0 nb	S.-H. Kim *et al.*[13]	$\sim$ 0.1 pb

Table 3: Summary of theoretical estimates for total cross sections of the $\pi^- p \to J/\psi n$ reaction at a center-of-energy of 4.4 GeV.

In general, meson-induced reactions exhibit larger cross sections than photoproduction reactions. This is because a meson initially contains $q\bar{q}$ content, while a photon must first convert into a $q\bar{q}$ pair before interacting with a target proton. To quantify this, we examine the cross section ratio of the pion-induced reaction to the photoproduction reaction, denoted as: $\mathscr{R} = \sigma(\pi^- p)/\sigma(\gamma p)$.

For comparison, we analyze the ϕ production reactions using both photon and pion beams. The ratio of these cross sections is approxiamtely 20. The total cross sections for

$\pi^- p \to \phi n$ reaction range from 19 to 25 μb in the beam momentum range from 1.6 to 2.0 GeV/c, whereas the near-threshold cross sections for ϕ photoproduction are roughly 1 μb.

Regarding J/ψ production, the GlueX Collaboration reported an approximate cross section of 0.7 nb for J/ψ photoproduction near $W = 4.4$ GeV. However, there is no experimental data available for near-threshold J/ψ production in the $\pi^- p$ reaction. Using two extreme theoretical estimates for the $\pi^- p \to J/\psi n$ cross section (0.1 pb and 50 nb), we can derive the ratio.

$$\mathscr{R}\Big|_{W=4.4\ \text{GeV}} = \frac{\sigma(\pi^- p \to J/\psi n)}{\sigma(\gamma p \to J/\psi p)} = \begin{cases} \dfrac{0.1\ \text{pb}}{0.7\ \text{nb}} = 1.4 \times 10^{-4} \\ \\ \dfrac{50\ \text{nb}}{0.7\ \text{nb}} = 71 \end{cases}$$

It is important to note that J/ψ production has not been observed in exclusive πN reactions. This proposal aims to achieve the world's first measurement of the near-threshold cross sections for the $\pi^- p \to J/\psi n$ reaction.

3 Experiment

We propose to measure exclusive J/ψ production in $\pi^- p$ reaction from threshold ($p_\pi = 8.2$ GeV/c) to a center-of-mass energy $W = 4.64$ GeV ($p_\pi = 11$ GeV/c). The high-momentum π^- beam is anticipated in the π20 beam line of the J-PARC Hadron Hall, as shown in Fig. 14(a). We will utilize the E50 dipole spectrometer [15], along with additional detector components. To achieve effective e/π separation at momenta above 4 GeV/c, we are considering the development of a new forward detector. This detector will cover the forward direction between two downstream hadron-blind detectors (HBD), and will feature a transition radiation detector and a lead glass calorimeter.

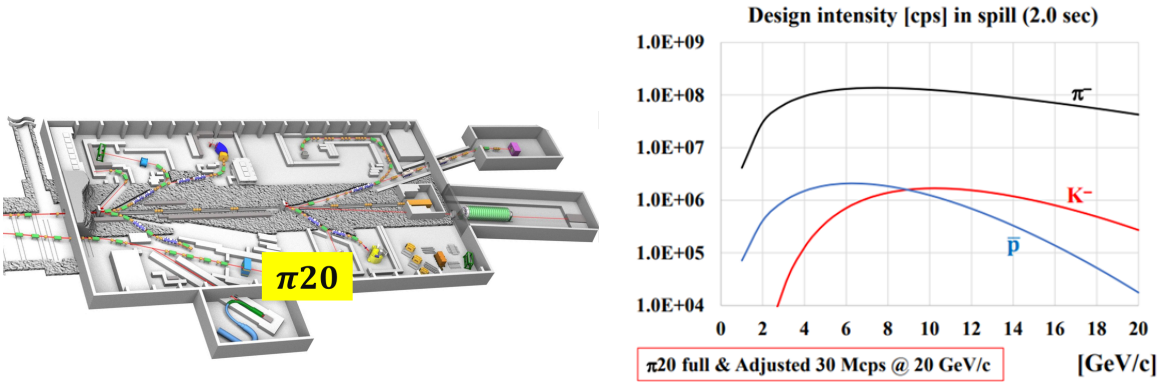

(a) (b)

Figure 14: Schematic of the π20 beam line in the Hadron Hall. (b) Estimated beam intensities of the π20 beam line for the 15 kW loss at the production target.

3.1 Beamline

A current Lambertson magnet system for the B line can deliver a π beam intensity of 10^5/spill in the momentum range of 2 to 20 GeV/c. In contrast, a future swinger magnet system is expected to provide a π beam intensity of up to 6×10^7/spill at 20 GeV/c, with a maximum loss of 15 kW. In the initial stages of its operation, it will start with a few 10^6/spill at a 1 kW loss, as shown in Fig. 14(b). The proposed experiment will use the π^- beam in the momentum range of 8.2 to 11 GeV/c, where the π^- beam intensity will reach 1×10^8/spill with a 2 s spill duration.

Dispersion matching of incident π^- beam trajectories enables a high beam momentum resolution of $\Delta p/p = 0.1\%(\sigma)$. This results in a 10 MeV/c resolution for a 10 GeV/c beam, and a 2 MeV resolution in the center-of-mass energy W for $\pi^- p$ reaction, This resolution is comparable to the single bin size of the $J/\psi p$ mass spectrum reported by the LHCb Collaboration. It is important to note that the single bin size of the $J/\psi p$ mass spectrum measured by GlueX is approximately 25 MeV.

3.2 The J/ψ Detector

The J/ψ detector will primarily utilize the E50 spectrometer, which includes fiber trackers, drift chambers, Cherenkov detectors, time-of-flight detectors, and muon detectors. The E50 detector offers larger acceptance and excellent particle identification capability.

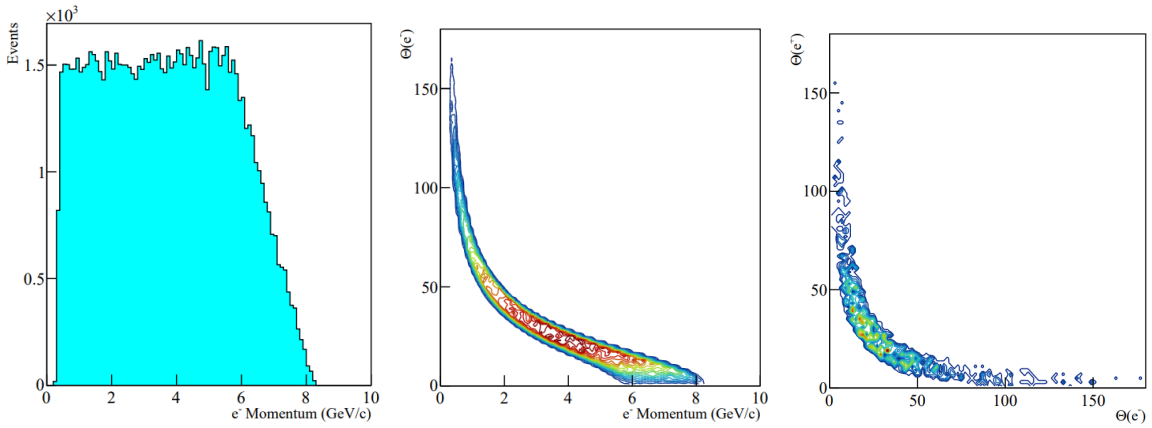

Figure 15: (a) Momentum distribution, (b) the correlation between momentum and decay angle, and (c) correlation between decay angles for $e^-(\mu^-)$ or $e^+(\mu^+)$ from J/ψ decays,

However, the electromagnetic decay of the J/ψ often produces e^+e^- with highly asymmetric momentum and angular distributions, as illustrated in Fig. 24. In the asymmetric decay of the $J/\psi \to e^+e^-$, a high-momentum electron tends to move in the forward direction, while a low-momentum positron spreads out over a larger angular region, and vice versa. The $J/\psi \to \mu^+\mu^-$ decay has a similar tendency in kinematics.

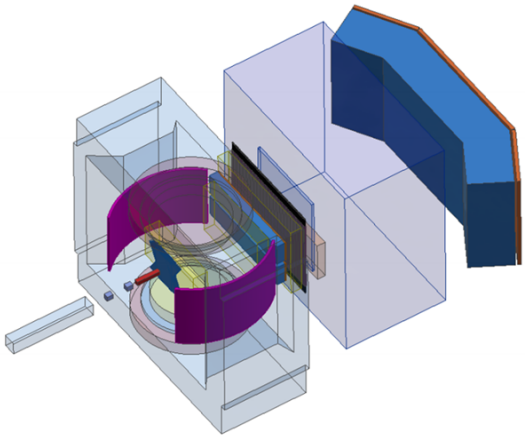

(a)

Detector Component	E50 (J/ψ)
Beam RICH	1
Fiber Tracker	2
Drift Chamber	3
TOF Array	2
Aeroge Cherenkov	1
RICH	1
μID RPC	1 (1+)
Transiton Radiation Detector	0 (1)

(b)

Figure 16: (a) Schematic of the J/ψ spectrometer and (b) a list of main detector components.

The E50 detector provides broad angular coverage from the LH_2 target, which allows it to capture a significant portion of the dilepton signals. However, to accurately identify the decays of e^+e^- and $\mu^+\mu^-$, additional particle identification detectors are necessary. In the case of the $J/\psi \to \ell^+\ell^-$ decay, the process is typically asymmetric; one of the decay leptons moves in the forward direction, while the other is emitted at a large angle.

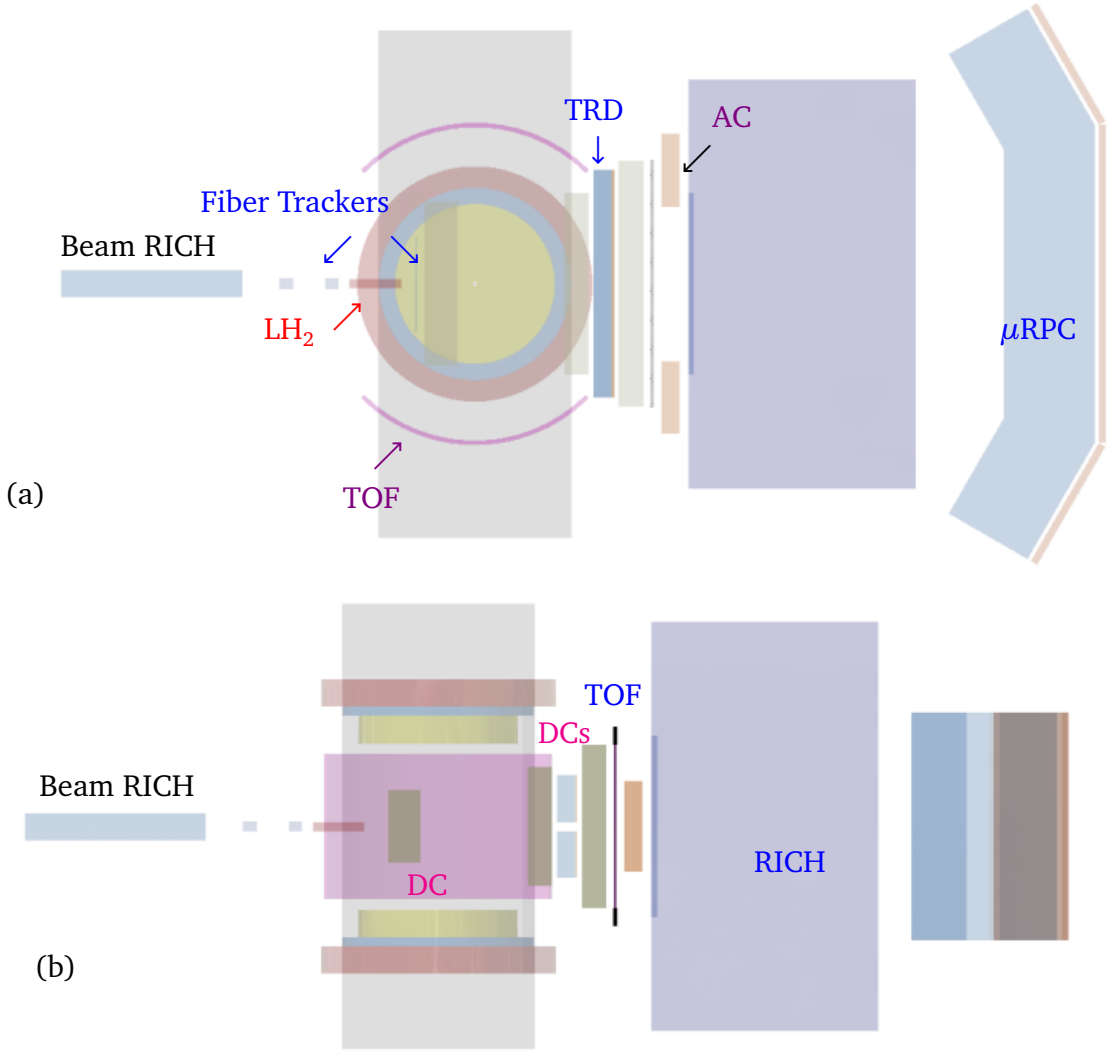

Figure 17: (a) Top view of the J/ψ detector and (b) its elevation view.

The J/ψ spectrometer, which is based on the E50 detector, is illustrated in Figs. 16 and 17. To achieve effective e/π separation, we are considering a transition radiation detector (TRD) as the most suitable option. We have initiated discussions for close collaboration with the GlueX team at Jefferson Lab. Their current prototype features a sensitive area of approximately 70×50 cm^2 and utilizes a TRD radiator with a 20 cm thick fleece and a triple GEM tracker. The TRD prototype is currently undergoing beam commissioning to ensure stable operation.

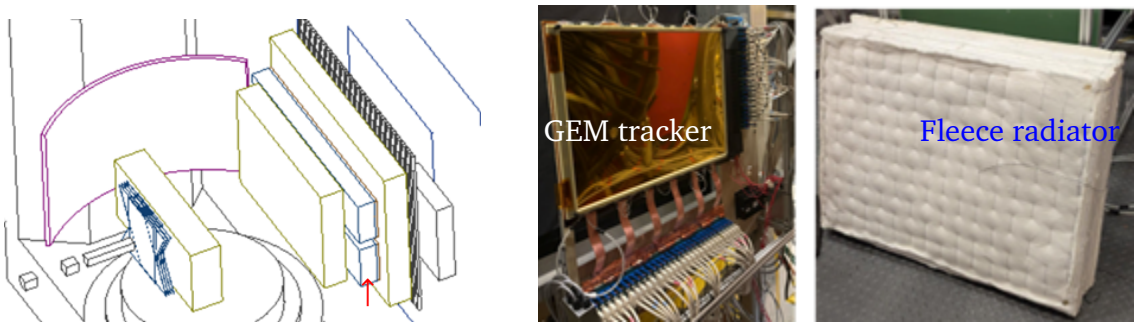

(a) (b)

Figure 18: (a) Location of the transition radiation detector and (b) photos of the TRD prototype under development by the GlueX team.

For detecting $J/\psi \to e^+e^-$ decays, two TRD modules will be positioned between two drift chambers near the exit of the magnet. These modules are separated vertically by a 5 cm gap to allow for beam passage. The coverage of the TRD is designed to match that of the forward drift chambers.

Detection of $J/\psi \to \mu^+\mu^-$ decays will be achieved using a large muon detector array, which consists of resistive plate chambers positioned behind a thick concrete wall. The current configuration of the E50 μRPC is flat and 3.5 m wide. We examined the optimal acceptance for two different configurations based on the current E50 design. In the flat configuration, the acceptance reaches saturation at approxminately 20% for widths exceeding 8 m, as illustrated in Fig. 19(a).

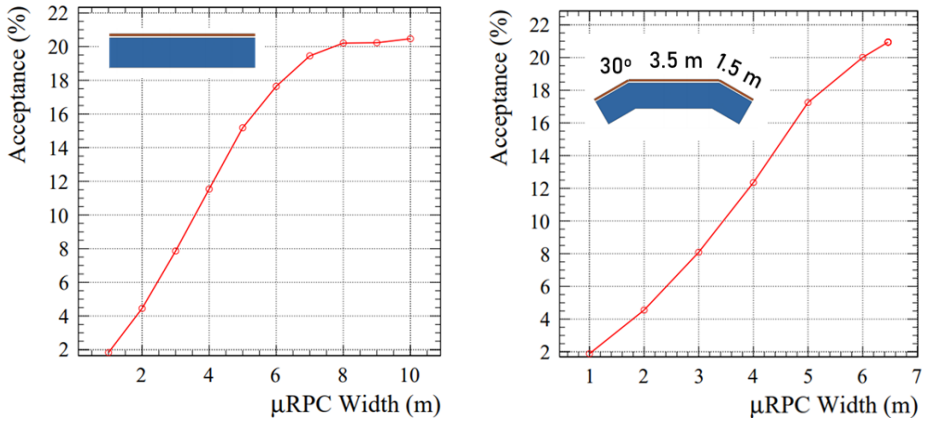

(a) (b)

Figure 19: (a) Acceptance with the width of the μRPC in (a) the flat configuration and (b) the two arm configuration.

The alternative configuration builds on the current flat design and includes two arms tilted at an angle of 30°. This design offers more effective coverage over a larger area. The 6 m width of this configuration achieves the same acceptance level as the 8 m wide

flat configuration, as shown in Fig. 19(b). Ultimately, we chose the second configuration, which consists of one flat section measuring 3.5 m and two angled arms, each 1.5 m wide.

The data acquisition (DAQ) will utilize a triggerless scheme in streaming mode. The development of this new DAQ system will be conducted in close collaboration with the E50 Collaboration and the SPADI Alliance.

3.3 Detector Simulations

We performed a Monte Carlo simulation for the $\pi^- p \to J/\psi n$ experiment. The event generator is based on the phase-space calculation for the $\pi^- p \to J/\psi n$ reaction followed by $J/\psi \to e^+e^-$ and $\mu^+\mu^-$ decays. A current simulation focuses on the feasibility study for reconstructing $J/\psi \to \ell^+\ell^-$ events from $\pi^- p$ reaction near the threshold. To access the total cross section, a broad angular coverage is critical across the energy region from threshold to $W = 4.64$ GeV.

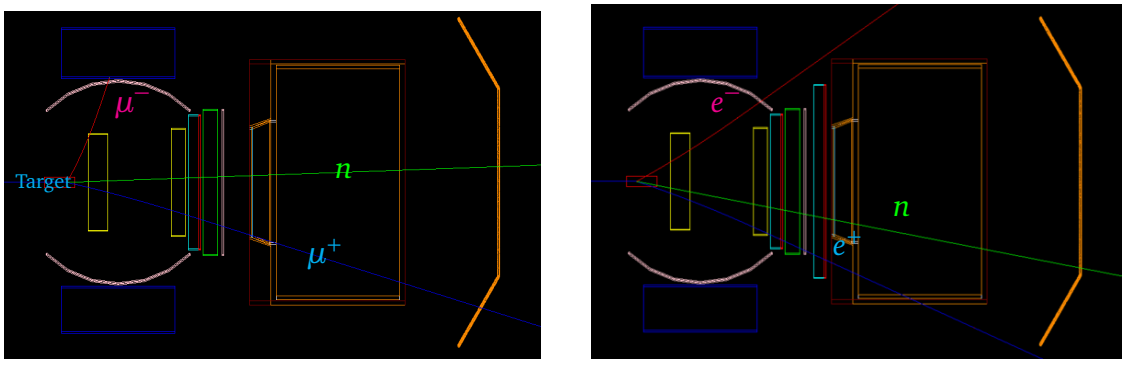

(a) (b)

Figure 20: Simulated events for the $\pi^- p \to J/\psi n$ reaction followed by (a) $J/\psi \to \mu^+\mu^-$ and (b) e^+e^- decays.

The typical simulated events for the $\pi^- p \to J/\psi n$ reaction are shown in Fig. 20(a) and (b), which depict the subsequent decays of $J/\psi \to \mu^+\mu^-$ and $J/\psi \to e^+e^-$, respectively. The opening angle between the two leptons is distributed across a broad range, and in most cases, at least one of the particles moves in the very forward direction.

The reconstructed distributions of $\cos\theta^*_{J/\psi}$ are shown in Figs. 21 and 22. For the $J/\psi \to \mu^+\mu^-$ decay, the event selection process requires the identification of at least one muon detected in the μRPC. To effectively suppress the background from multipion processes, we limit our reconstruction to only two oppositely charged tracks.

There may be background contributions associated with beams, such as the decays of $\pi^- \to \mu^- \bar{\nu}_\mu$. Additionally, the multipion production reaction could influence the measurement of $\mu^+\mu^-$ pairs when one of the final-state pions decays into muons. We considered a scenario in which one signal muon is correctly identified while the other muon, originating from background processes, is accidentally detected, Fig. 23(a) and (c) display the

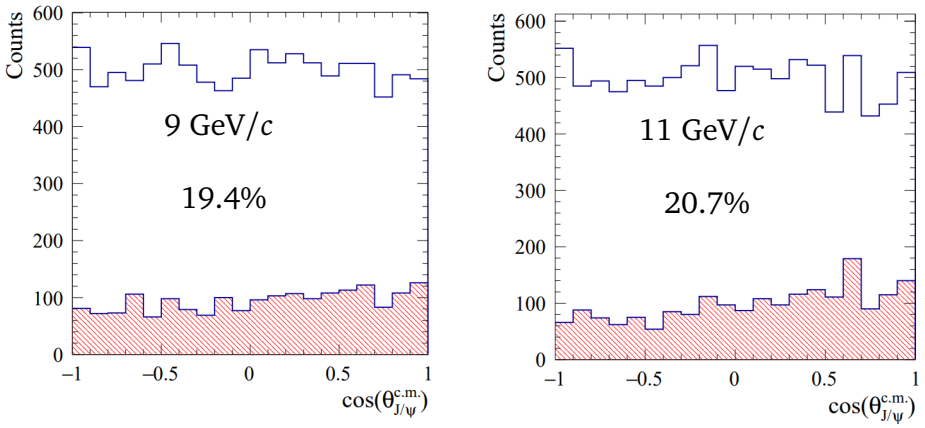

(a) (b)

Figure 21: Simulated angular distributions for the $\pi^- p \to J/\psi n$ reaction, followed by the $J/\psi \to \mu^+\mu^-$ decay at 9 GeV/c (a) and 11 GeV/c (b) are presented. The blue histograms represent the generated distributions, while the red ones show the accepted distributions.

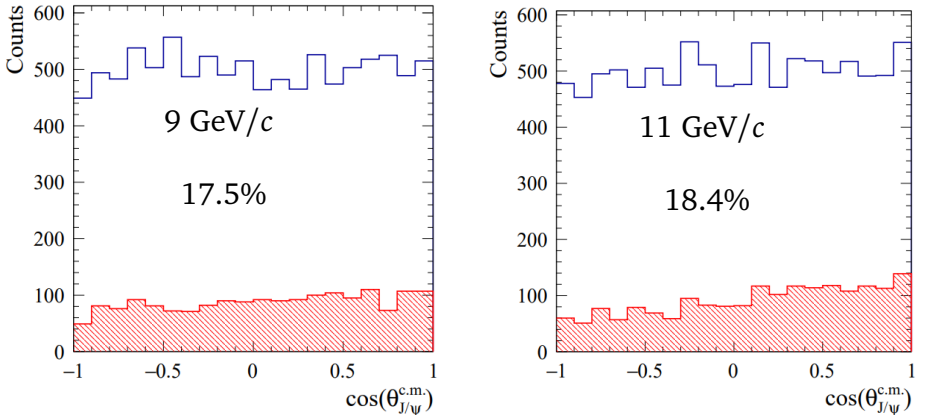

(a) (b)

Figure 22: Simulated angular distributions for the $\pi^- p \to J/\psi n$ reaction, followed by the $J/\psi \to e^+e^-$ decay at 9 GeV/c (a) and 11 GeV/c (b) are presented. The blue histograms represent the generated distributions, while the red ones show the accepted distributions.

reconstructed $\mu^+\mu^-$ mass spectra for the J/ψ and accidentally misidentifed $\mu^+\mu^-$ pairs. In contrast, Fig. 23(b) and (d) illustrate the missing mass spectra for the $p(\pi^-, \mu^+\mu^-)X$ reaction, where a peak corresponding to the neutron is observed.

For the $J/\psi \to e^+e^-$ decay, we impose an event selection criteria that requires at least one of the particles, e^+ or e^-, to be identified in transition radiation detectors. Charged particles emit transition radiation when the Lorentz factor $\gamma >\sim 1000$. Therefore, as demonstrated in Fig. 24(a) and (c), pions do not emit radiation in the energy region of this experiment. The effective operation of the transition radiation detector in ALICE indicates a strong pion suppression factor, ranging from 10^-3 to 10^-2. We anticipate that

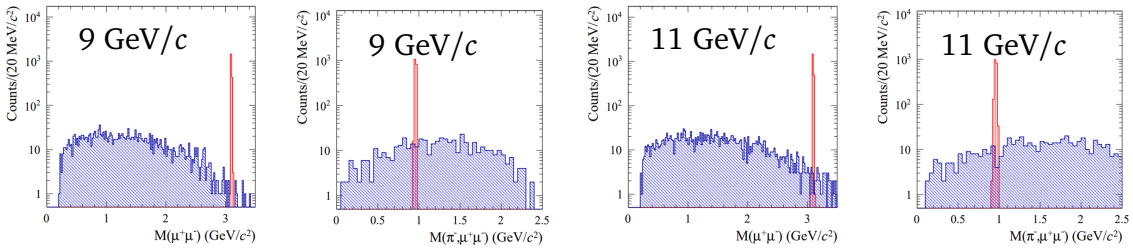

(a) (b) (c) (d)

Figure 23: Reconstructed $\mu^+\mu^-$ mass and missing mass distributions for the $\pi^- p \to J/\psi n$ reaction, followed by the $J/\psi \to \mu^+\mu^-$ decay at 9 GeV/c ((a) and (b)) and 11 GeV/c ((c) and (d)) are presented. The blue histograms represent contributions from $\pi^- p \to \pi^+\pi^- n$ reaction, which are accidentally reconstructed.

two independent TRDs can significantly enhance the e/π separation.

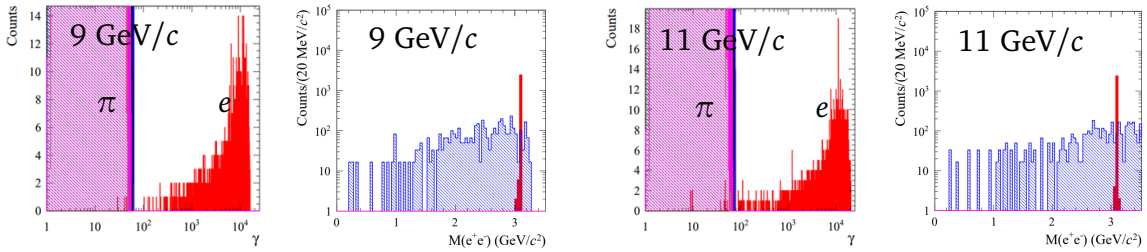

(a) (b) (c) (d)

Figure 24: Calculated Lorentz factor γ and reconstructed e^+e^- mass distributions for the $\pi^- p \to J/\psi n$ reaction, followed by the $J/\psi \to e^+e^-$ decay at 9 GeV/c ((a) and (b)) and 11 GeV/c ((c) and (d)) are presented. The blue histograms represent contributions mostly from $\pi^- p \to \pi^+\pi^- n$ reaction, which are accidentally reconstructed.

Additionally, we are also considering alternative detectors for redundant electron identification, such as electromagnetic calorimeters and a low-pressure gas Ring Imaging Cherenkov (RICH) detector. A large preshower calorimeter array can be placed between the RICH and the μRPC. Consequently, the reconstructed e^+e^- mass distributions are presented in Fig. 24(b) and (d). Among multipion production processes, only the $\pi^- p \to \pi^+\pi^- n$ reaction can survive.

3.4 Expected Yield of $\pi^- p \to J/\psi n$ Events

The expected yield (Y) for J/ψ production events can be estimated as:

$$\begin{aligned} Y &= (2.5\times10^{7}(\mathrm{s}^{-1})\cdot 2.4\times10^{24}(\mathrm{cm})^{-2})\cdot\sigma_{tot}\cdot\mathscr{B}(J/\psi\to\ell^+\ell^-)\cdot\varepsilon_{\mathrm{acc}}\cdot\varepsilon_{\mathrm{rec}} \\ &= 6\times10^{-2}/\mathrm{s}\cdot\sigma_{\mathrm{tot}}(\mathrm{nb})\cdot\cdot\mathscr{B}(\mathrm{J}/\psi\to\ell^+\ell^-)\cdot\varepsilon_{\mathrm{acc}}\cdot\varepsilon_{\mathrm{rec}} \\ &= 620/\mathrm{d}\cdot\sigma_{\mathrm{tot}}(\mathrm{nb})\cdot\varepsilon_{\mathrm{acc}}\cdot\varepsilon_{\mathrm{rec}}, \end{aligned}$$

where $\mathscr{B}(J/\psi \to \ell^+\ell^-)$ denotes the branchng ratio of the $J/\psi \to \ell^+\ell^-$ decay involving $\mu^+\mu^-$ and e^+e^- channels, which are 5.961% and 5.971%. The beam intensity of 10^8/spill in a 2 s spill duration corresponds to a beam rate of 2.5×10^7/s. A liquid hydrogen (LH_2) target of 57 cm in length gives an areal density of 4 g/cm^2, and corresponds to the number of target protons, 2.4×10^{24}(cm^{-2}). The total cross section σ(nb) is the value in the unit of nanobarns. The acceptance $\varepsilon_{\rm acc}$ is obtained as roughly 20%, and the reconstruction efficiency is assumed to be 50%. Consquently, the expected yield for $J/\psi \to \ell^+\ell^-$ events will be approximately 62 in a day per nanobarn, or 250 for $\sigma = 4$ nb (an average value taken from Fig. 7). The cross section measurement should cover the range of roughly 0.6 GeV between threshold and 4.64 GeV.

4 Beam Time Request

We plan to conduct a measurement of the $\pi^- p \to J/\psi n$ reaction in the momentum range of 8.2 GeV to 11.0 GeV/c, with 0.02 GeV/c increments. We will then measure the total cross sections at 30 energy points to observe the general trend of the lineshape. To explore the detailed lineshapes near the open-charm mass thresholds and the masses of $P_{c\bar{c}}$ states, we need to measure the cross sections with 4 MeV/c intervals at six regions, which will add additional 30 energy points.

As a result, we request two separate beam times, each of 50 days. The first beam time will be dedicated to provide the first-ever data of the near-threshold J/ψ production in $\pi^- p$ reaction. We will request the second beam time for precise cross section measurements near the $P_{c\bar{c}}$ states, if the first dataset supports the emergene of intriguing peaking structures.

5 Costs and Manpower

The development of the new detector components for the J/ψ detector, as well as travel expenses and manpower, will be covered by current and future research grants. The manpower will include the J/ψ Collaboration and new members with particular expertise in exploring the J/ψ mesons in different reactions and utilizing a π^- beam. The experts from the high-p beam line will help in preparing this proposed experiment, which is crucial in assessing the beam line information.

6 Summary

We propose a new experiment to study J/ψ production in $\pi^- p$ reactions near the threshold at the π20 beam line. J/ψ production in the π^-p reaction will provide insights into the nature of $c\bar{c}$ pair creation in pion-induced reactions, particularly regarding hidden-charm pentaquark states.

We plan to measure the total cross sections for the exclusive $\pi^- p \to J/\psi n$ reaction near the threshold using the E50 spectrometer, enhanced by additional forward detector components. Our experimental setup will be prepared in close collaboration with the E50 Collaboration.

This measurement will provide the first-ever data on π^--induced J/ψ production reaction near the threshold. We are requesting 50 days of beam time for the energy scan. If we discover new structures related to exotic pentaquark states, we will request an additional 50 days to investigate pentaquark searches at finer energy intervals.

References

[1] R. Aaji *et al.* (LHCb Collaboration), Phys. Rev. Lett. 122001 (2019).

[2] R. Aaji *et al.* (LHCb Collaboration), Phys. Rev. Lett. 128, 062001 (2022).

[3] S. Adhikari *et al.* (GlueX Collaboration), Phys. Rev. C 108, 025201 (2023).

[4] I. Strakovsky *et al.*, Phys. Rev. C 108, 015202 (2023).

[5] S. Navas *et al.* (Particle Data Group), Phys. Rev. D 110, 030001 (2024) and 2025 updates.

[6] M.-L. Du *et al.,* Eur. Phys. J C**80**, 1053 (2020).

[7] S. Clymton, H.-Ch. Kim, and T. Mart, `arXiv:2408.04166` (2024).

[8] I.-H. Chiang *et al.*, Phys. Rev. D34, 1619 (1986).

[9] K. Jenkins *et al.*, Phys. Rev. D17, 52 (1978).

[10] A. Sibirtsev and K. Tsushima, `nucl-th/9810029` (1998).

[11] Q.-F. Lü *et al.*, Phys. Rev. D 93, 034009 (2016).

[12] J.-J. Wu and T.-S. H. Lee, Phys. Rev. C 88, 015205 (2013).

[13] S.-H. Kim, H.-Ch. Kim and A. Hosaka, Phys. Lett. B 763, 358 (2016).

[14] H. Courant *et al.*, Phys. Rev. D 16, 1 (1977).

[15] H. Noumi, J-PARC E50, Charmed baryon spectroscopy via the (π, D^*) reaction.